Fermi National Accelerator Laboratory

FERMILAB-Conf-86/97-E
7180.605

PRODUCTION OF HADRONS AND LEPTONS AT HIGH p_t AND PAIRS AT HIGH MASS*

Charles N. Brown
Fermi National Accelerator Laboratory, Batavia, IL 60510 USA

and

Daniel M. Kaplan
Florida State University, Tallahassee, FL 32306 USA

and

the E-605 collaboration†: CERN, Columbia, Fermilab, Florida State, KEK, Kyoto, Saclay, SUNY/Stony Brook, U. of Washington

May 1986

*Talks given at the Aspen Physics Institute, Aspen, Colorado, January, 1986, and the Seventh Vanderbilt High Energy Physics Conference, Nashville, Tennessee, May 15 - 17, 1986

Production of Hadrons and Leptons at High p_t and Pairs at High Mass

Charles N. Brown, Fermilab, Batavia, IL 60510,

Daniel M. Kaplan, Florida State University, Tallahassee, FL 32306,

and the E605 collaboration[†]: CERN, Columbia, Fermilab, Florida State, KEK, Kyoto, Saclay, Stony Brook, U. of Washington

(Talks given at the Aspen Physics Institute, Jan. 1986, and the Seventh Vanderbilt High Energy Physics Conference, May 1986)

1 Introduction

The study of particle production at high transverse momentum (p_t) and pair production at high mass in energetic collisions between nucleons has been a fruitful area of research for over a decade [1-3]. The approach goes back to Rutherford [4] and is based on the notion that scattering at high momentum-transfer should reveal the internal structure of the scatterers. Nowadays these processes are analyzed in terms of the parton model and Quantum Chromo-Dynamics (QCD). Previous experiments by this collaboration confirmed the parton-scattering model of large-p_t and high-mass production [2] and discovered the T particles [3] and the fifth quark. The present experiment extends these measurements to higher beam energy and improves resolution, particle identification, and luminosity. Besides addressing QCD issues, the data also allow limits to be set on the mass and lifetime of the axion.

2 Apparatus

Experiment 605 at Fermilab uses a large spectrometer designed to distinguish accurately pions, kaons, protons, electrons, and muons and make precise measurements of their trajectories in the region near 90° in the center-of-momentum frame of the colliding nucleons. Measurements extend from a few GeV/c transverse momentum out to near the kinematic limit. The large "SM12" magnet (see Figure 1) deflects high-p_t charged particles around the beam dump and into the sensitive volume of the detectors, while neutral particles produced in the target are absorbed in the dump or in the magnet walls and shielding. Charged-particle trajectories are measured at three detector stations by proportional and drift chambers, and consistency of the trajectory upstream and downstream of the "SM3" magnet verifies that the particle was produced in the target. Scintillation-counter hodoscopes at the three stations furnish a crude measurement of the trajectory for triggering purposes. Particle identification is provided by the ring-imaging Cherenkov counter [5], the electron and hadron calorimeters, and the muon proportional tube arrays located behind the

calorimeters and additional shielding. The large p_t kick of SM12 (8 GeV/c at full excitation) combined with the good resolution of the drift chambers (200 μm r.m.s) yields mass resolution better than 0.2% r.m.s. at m = 10 GeV/c^2.

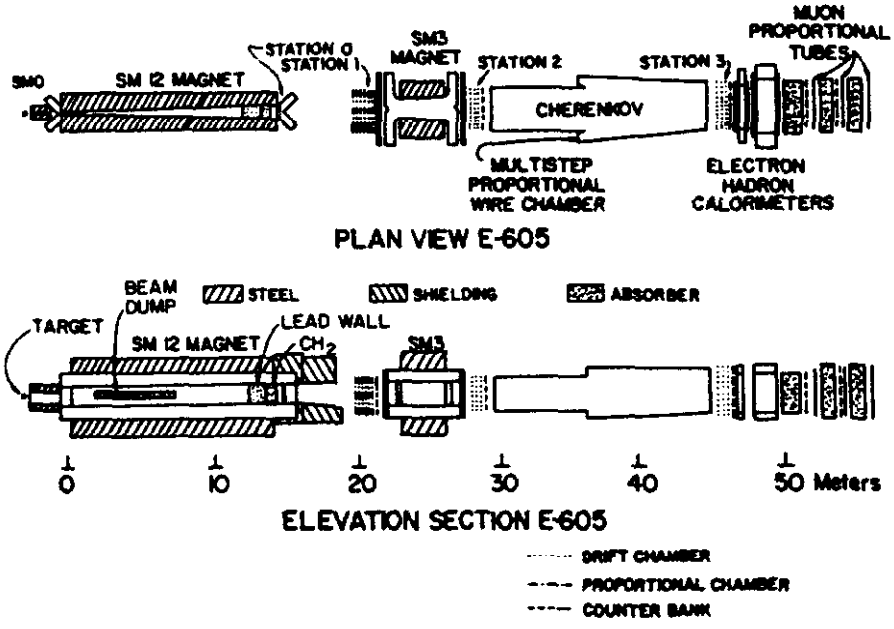

FIGURE 1: Plan and elevation of the apparatus, showing Pb absorber and Station 0 chamber which were added for the 1985 run.

3 Rate Limitations and Chronology of Runs

Luminosity was limited by counting rates in the detectors. The main problem was production of neutrals in the walls of SM12, which could then illuminate the detectors (see Figure 2). During our first run, in the Spring of 1982, this background limited our luminosity to 3 x 10^{34} $cm^{-2}s^{-1}$. The next run took place in the Winter of 1984; this was the first run of the Tevatron, but at a beam energy of 400 GeV. In preparation for this run we lined the inner walls of SM12 with carefully designed Pb and W absorbers and were thus able to operate at 10^{35} $cm^{-2}s^{-1}$. Finally, in 1985 we erected a 4'-thick Pb wall at the exit of SM12 and concentrated on dimuon measurements at a luminosity of 3 x 10^{36} $cm^{-2}s^{-1}$. Data were taken using a variety of targets in order to study nuclear effects. Table 1 gives the integrated luminosities for each run and target. To date, only the 1982 data have been fully analyzed [6,7], but preliminary results from the 1984 and 1985 runs will also be presented.

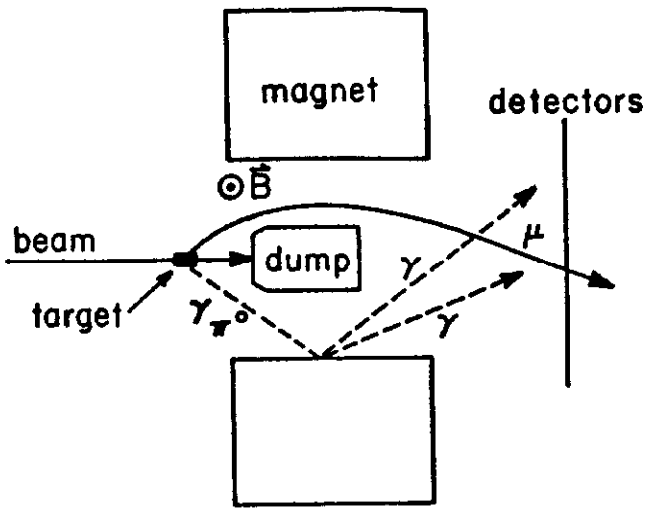

FIGURE 2: Schematic diagram of apparatus illustrating photon background problem.

TABLE 1: Data Recorded

	Integrated Luminosity/Nucleon (10^{39} cm^{-2})						
	target					$\sqrt{s}$ (GeV)	aperture
	Be	Cu	W	LH_2	LD_2		
1982	0.2	0.3	0.3			27.4	open
1984	1.5	2.2	3.5	0.7	2.6	27.4	open
"	12.9		2.2	0.8		38.8	open
1985		2800				38.8	closed

4 Nuclear Effects

The differential cross-section vs. p_t has been observed to depend in a complicated way on the atomic weight (A) of the target nucleus. The dependence might be expected to be exponential in A, with exponent $\alpha = 2/3$ if the nucleons on the surface of the nucleus shadow nucleons in the interior, or with $\alpha = 1$ if there is no shadowing. The former case would be expected (and has been observed) at low p_t (<1 GeV/c), where interaction cross-sections are large and so there is significant absorption of the incident nucleon as it penetrates a nucleus, but at high p_t (>1 GeV/c) one is sensitive to processes involving hard scattering of partons and small interaction cross-sections, so α should approach 1.

The observation [1] of $\alpha > 1$ at $p_t > 2$ GeV/c suggests that collective behavior of nucleons in the target nucleus is being observed. Multiple hard scattering of partons is capable of explaining these results, at least at a qualitative level. Figure 3 shows our single-hadron data [7] (from the 1982 run) and data from the Chicago-Princeton [1] and Columbia-Fermilab-Stony Brook collaborations [8], along with predictions of the constituent multiple scattering (CMS) model of Lev and Petersson [9]. The model is seen to reproduce the trend of the data, though there is some disagreement in detail.

A further prediction of the CMS model is independence of α on mass for symmetric hadron-pair production, since symmetric hadron pairs tend to arise from single hard scatters. This prediction is borne out by the data, as shown in Figure 4. For fixed mass, α should rise as the net p_t of the pair increases. Our acceptance for net $p_t \neq 0$ is small in the (approximately vertical) production plane, however we can define p_{out} as the momentum component of one hadron perpendicular to the plane defined by the beam direction and the momentum vector of the other hadron. According to the CMS picture, α should rise with increasing p_{out}, since multiple scatters are required to give a momentum component out of the plane. Figure 5 bears out this prediction.

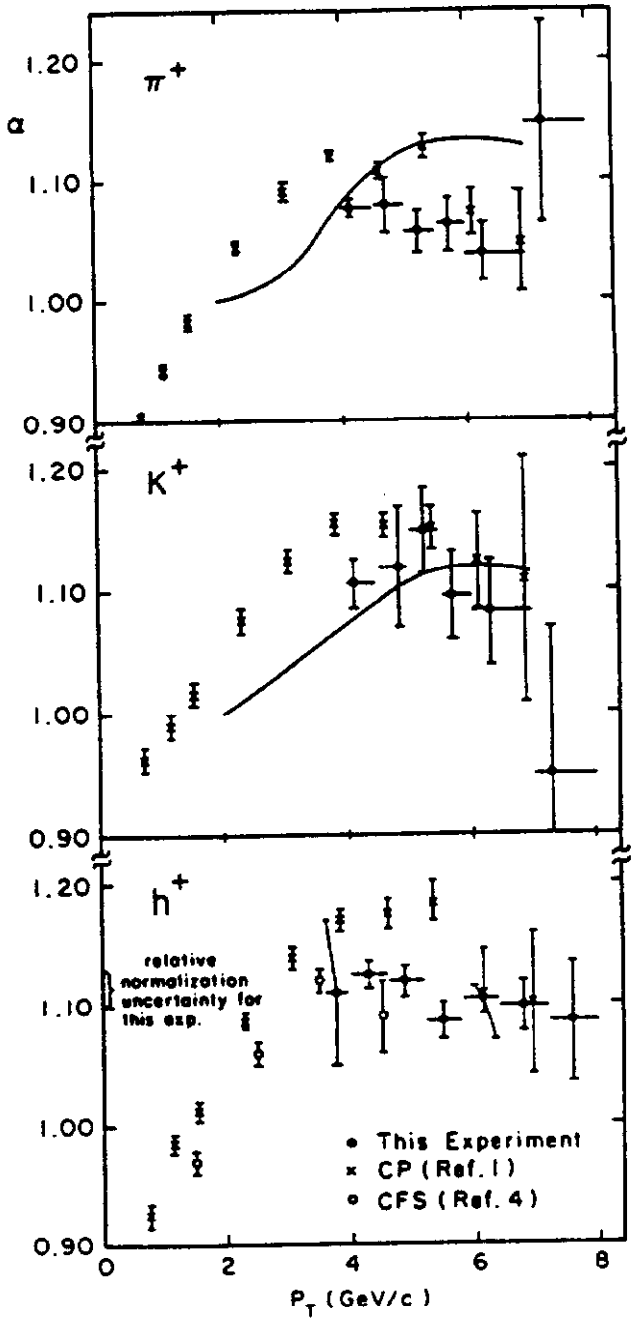

FIGURE 3: The exponent α of the A-dependence of positive-hadron production cross-sections at 400 GeV vs. p_t; the curves indicate the predictions of the constituent multiple scattering model for π^+ and K^+ production.

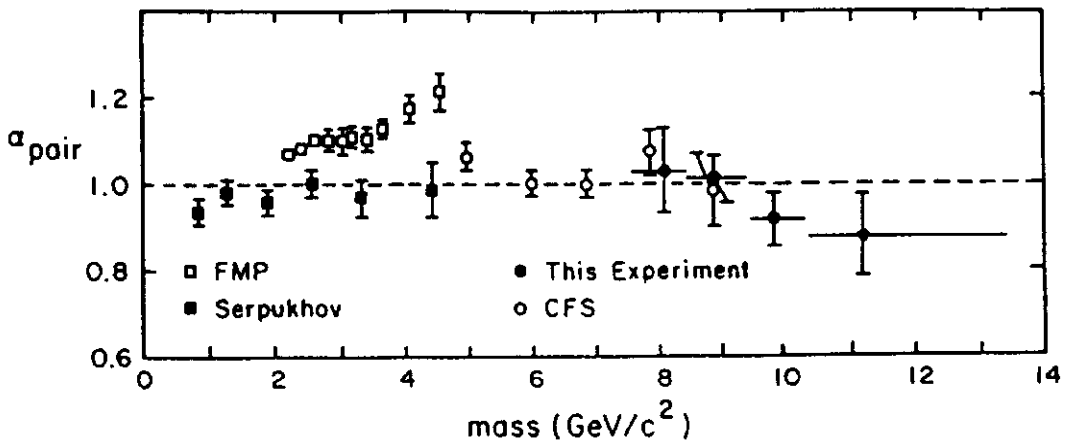

FIGURE 4: The exponent α of the A-dependence of the hadron-pair production cross-section at 400 GeV vs. pair mass.

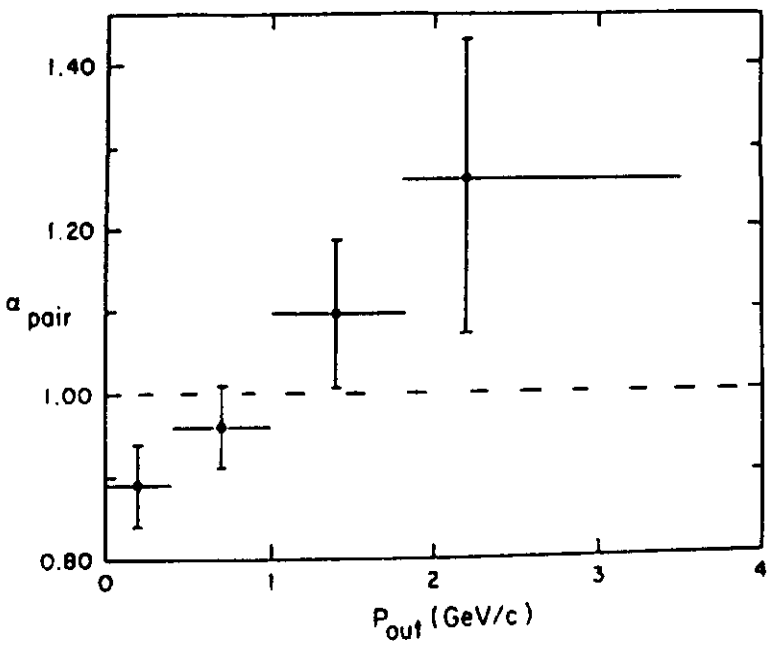

FIGURE 5: The exponent α of the A-dependence of the hadron-pair production cross-section at 400 GeV vs. P_{out}.

5 Cross-Sections vs. p_t and θ

The magnitude and shape of hadron production cross-sections at large p_t vs. p_t and scattering angle θ are calculable from QCD, given some information about how the scattered partons fragment into the observed particles. We have used the Lund monte carlo [10] to perform such a calculation, using the PYTHIA (4.2) and JETSET (6.2) routines to model parton scattering and fragmentation. Figure 6 shows the inclusive invariant cross-section vs. p_t to produce positive hadrons, compared with the Lund monte carlo prediction. The shapes are seen to agree well, however the magnitude of the Lund prediction is too low by a factor of 2.6.

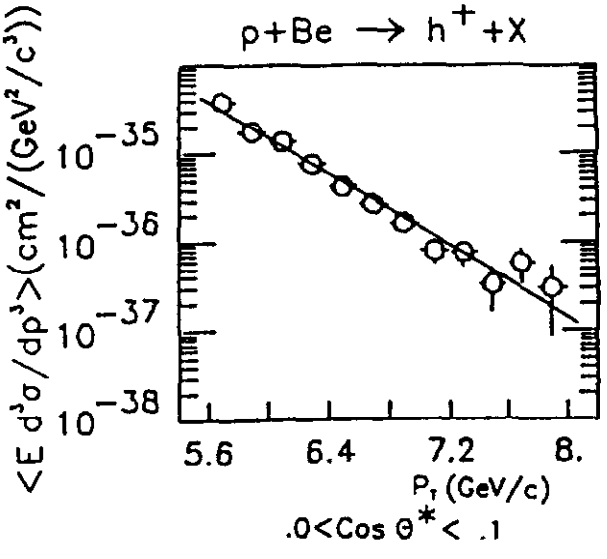

FIGURE 6: Inclusive invariant cross-section vs. p_t for positive hadron production off of Be at 400 GeV; the curve represents the Lund monte carlo prediction, multiplied by 2.6.

The dependence of the cross-section on θ has not been measured by any previous experiment in this range of p_t and θ. Figure 7 presents the power α of the atomic-weight dependence vs. cos θ, as measured in our 1982 run using Be, Cu, and W targets. The data are consistent with a constant value of α in our range of cos θ. Figures 8 and 9 present the invariant cross-sections vs. cos θ for positive and negative hadrons from the three targets. We show also an extrapolation to A = 2 (labeled "deuterium"), compared with QCD predictions from the Lund monte carlo and from a calculation to leading-log order by J.F. Owens [11]. The Lund prediction has been multiplied by 2.6 to facilitate the comparison, but the leading-log prediction agrees in magnitude with the experimental results.

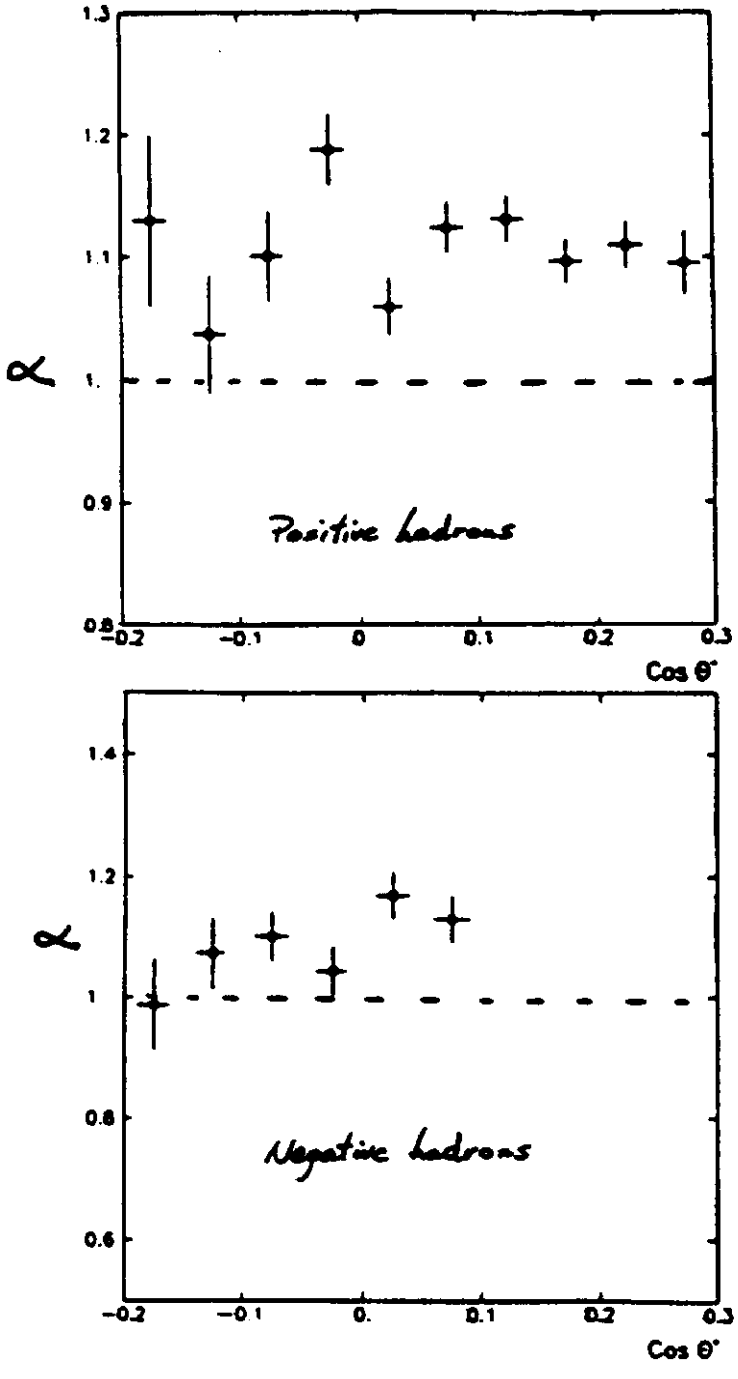

FIGURE 7: The power α of the A-dependence of positive- and negative-hadron production cross-sections vs. cos θ.

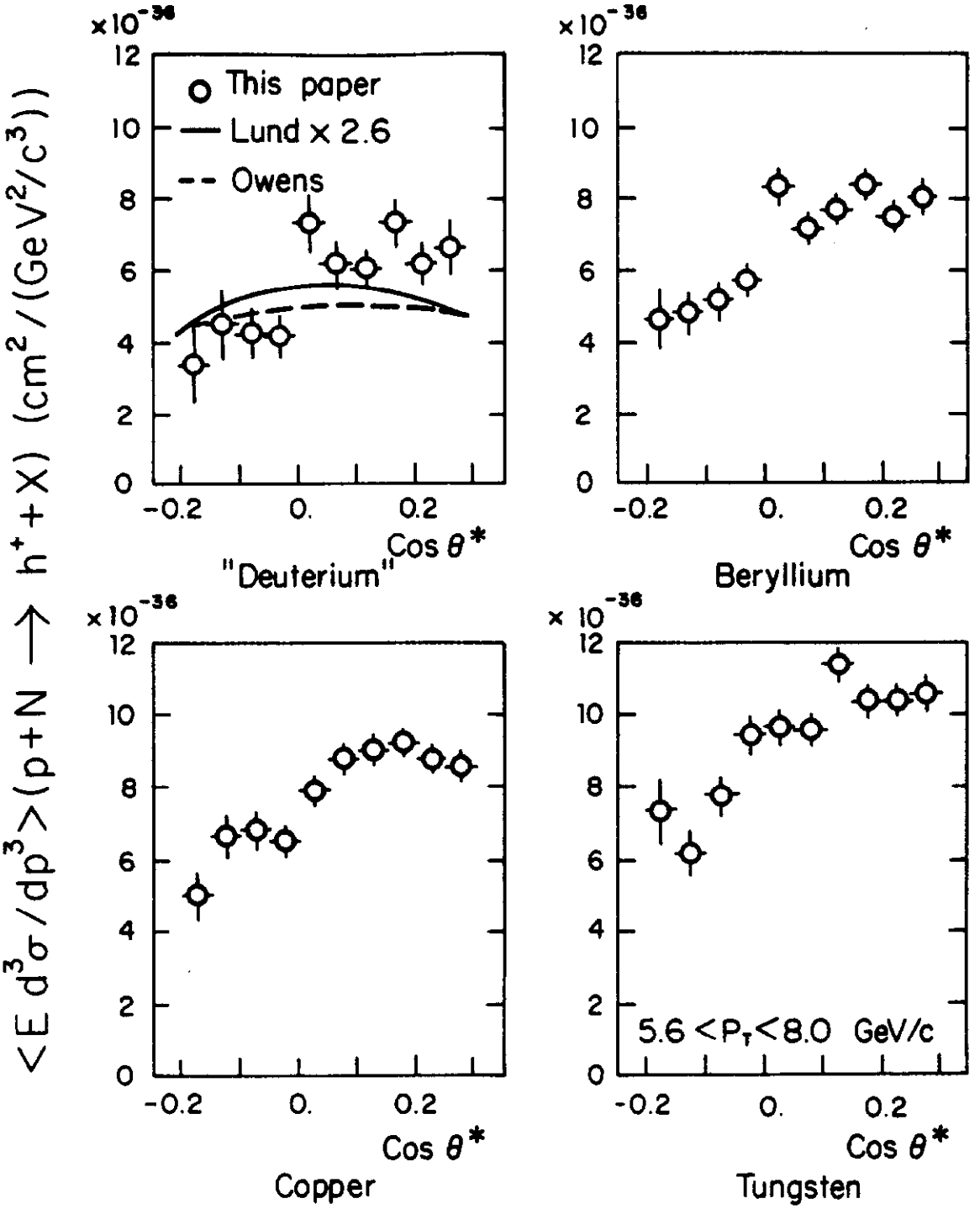

FIGURE 8: The invariant cross-section vs. cos θ for positive hadron production at 400 GeV off Be, Cu, and W targets, and its extrapolation to A = 2 ("Deuterium").

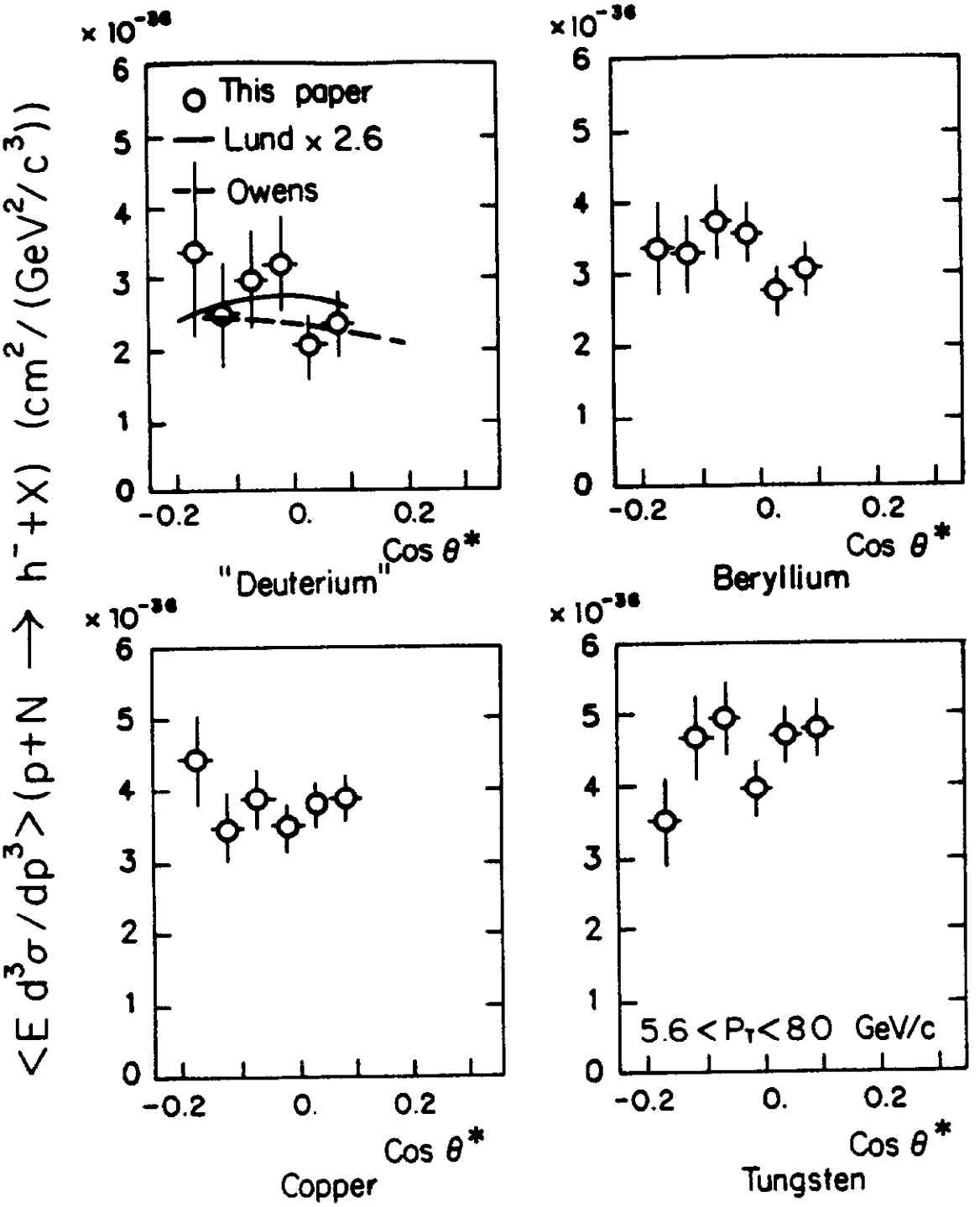

FIGURE 9: The invariant cross-section vs. cos θ for negative hadron production at 400 GeV off Be, Cu, and W targets, and its extrapolation to A = 2 ("Deuterium").

For positive hadrons, both the data and the QCD predictions show an enhancement at angles forward of 90°, but the data show a stronger enhancement than either calculation. This forward enhancement arises in the QCD models due to the presence of neutrons in the target, as follows: At these high values of $x_t = 2p_t / \sqrt{s}$, the cross-section is dominated by scattering of valence quarks off of each other and off of gluons; also u quarks tend to fragment into positive hadrons, whereas d quarks tend to fragment into negative hadrons. Since the u-quark structure function is harder in the proton and the d-quark structure function is harder in the neutron, in proton-neutron collisions positive hadrons tend to be produced in the proton direction (forwards) and negative hadrons in the neutron direction (backwards).

Note that the results heretofore presented are all based on the 1982 run. Once the analysis of the 1984 data is complete we will have better statistics by an order of magnitude, as well as better acceptance and better control over systematic errors. Some preliminary results from the 1984 data are presented below.

6 Particle Ratios

Figure 10 presents preliminary measurements of particle production ratios at 400 GeV using the LH_2 target, along with results from the Chicago-Princeton collaboration and Lund monte carlo predictions. The two data sets are in agreement where they overlap, and both agree with the Lund prediction for π^+/π^-, however the Lund monte carlo is seen to underestimate production of kaons and overestimate baryon production. These predictions are sensitive to two parameters in the fragmentation model: the ratio of s to u quark production and the ratio of diquark to single quark production. These parameters were determined from e^+e^--annihilation data [12] to be 0.3 and 0.1 (respectively); our data prefer the values 0.5 and 0.05. Similar problems have been noted by two ISR experiments [13] (at lower values of x_t). Note that both the data and the monte carlo runs suffer limited statistics so far.

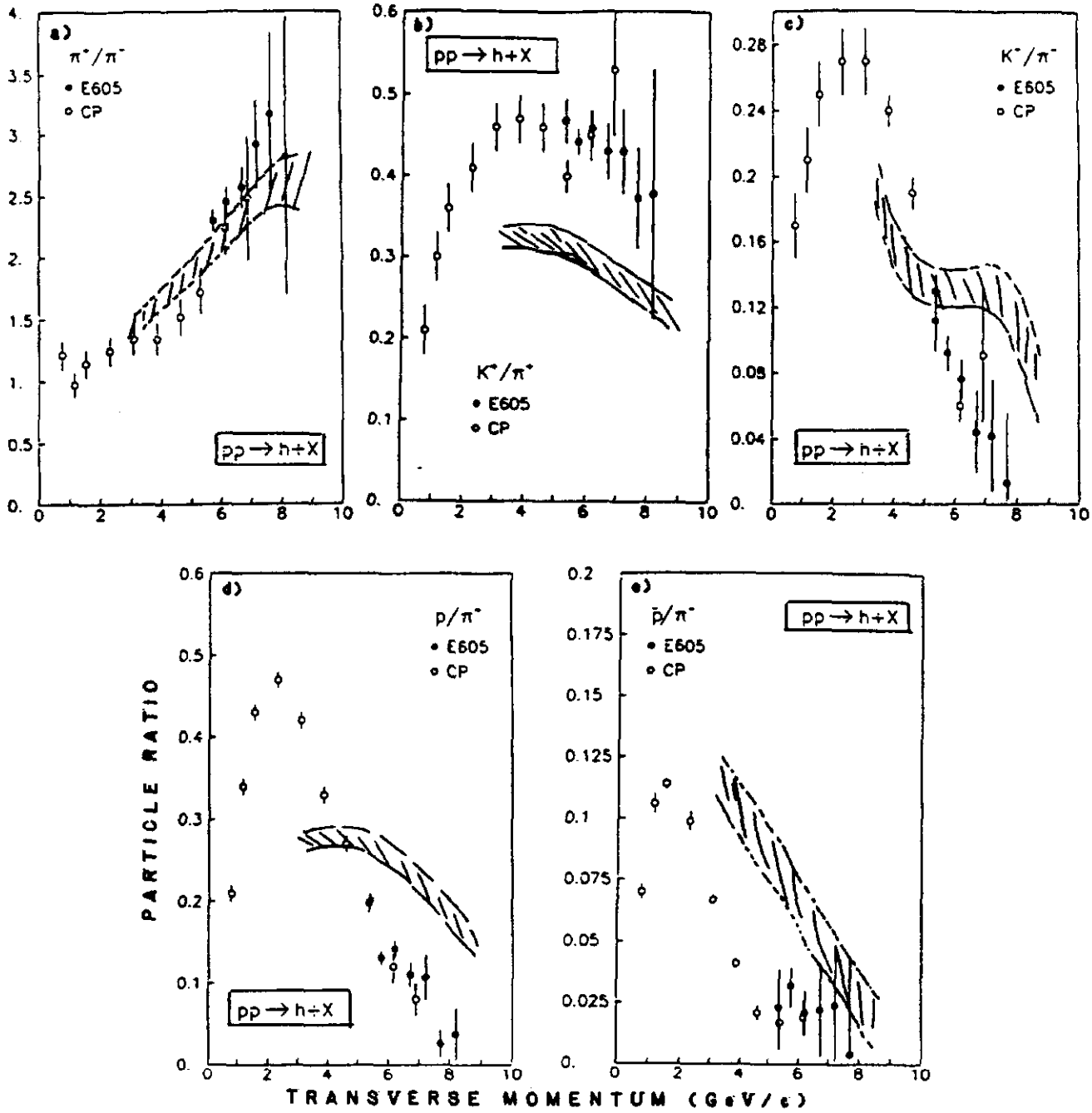

FIGURE 10: Invariant-cross-section ratios for pions, kaons, and protons produced in 400 GeV p-p collisions: a) π^+/π^-, b) K^+/π^+, c) K^-/π^-, d) p/π^+, and e) $\bar{p}/\pi^-$. The shaded bands represent the Lund monte carlo predictions.

7 800 GeV Data

7.1 Open-Aperture Run

Figure 11 presents preliminary results on the yields vs. p_t of positive hadrons and hadron pairs at 800 GeV off of Be. The results shown represent the first 3% of data taken and serve to indicate the quality of the results expected once the analysis is complete.

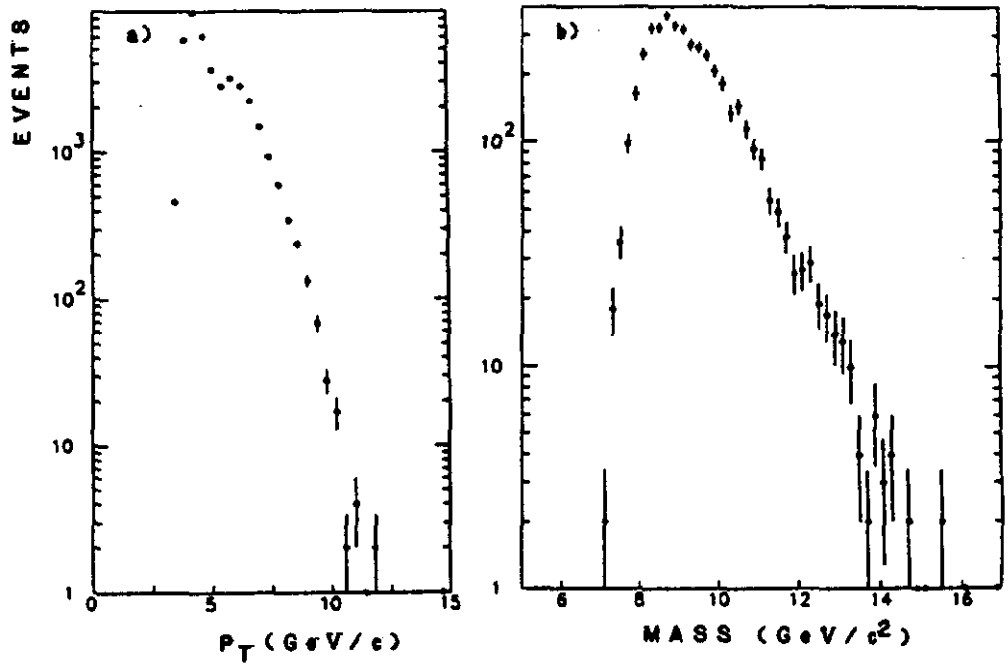

FIGURE 11: Yield of a) positive hadrons vs. p_t and b) opposite-sign hadron pairs vs. mass at 800 GeV off Be for first 3% of data taken.

Figure 12 shows the dimuon and dielectron yields vs. mass. The T states are clearly resolved, and the yields in the two modes are equal to within 20%. No large opposite-sign μe signal is seen; the yield is less than 1% of the dimuon and dielectron yields.

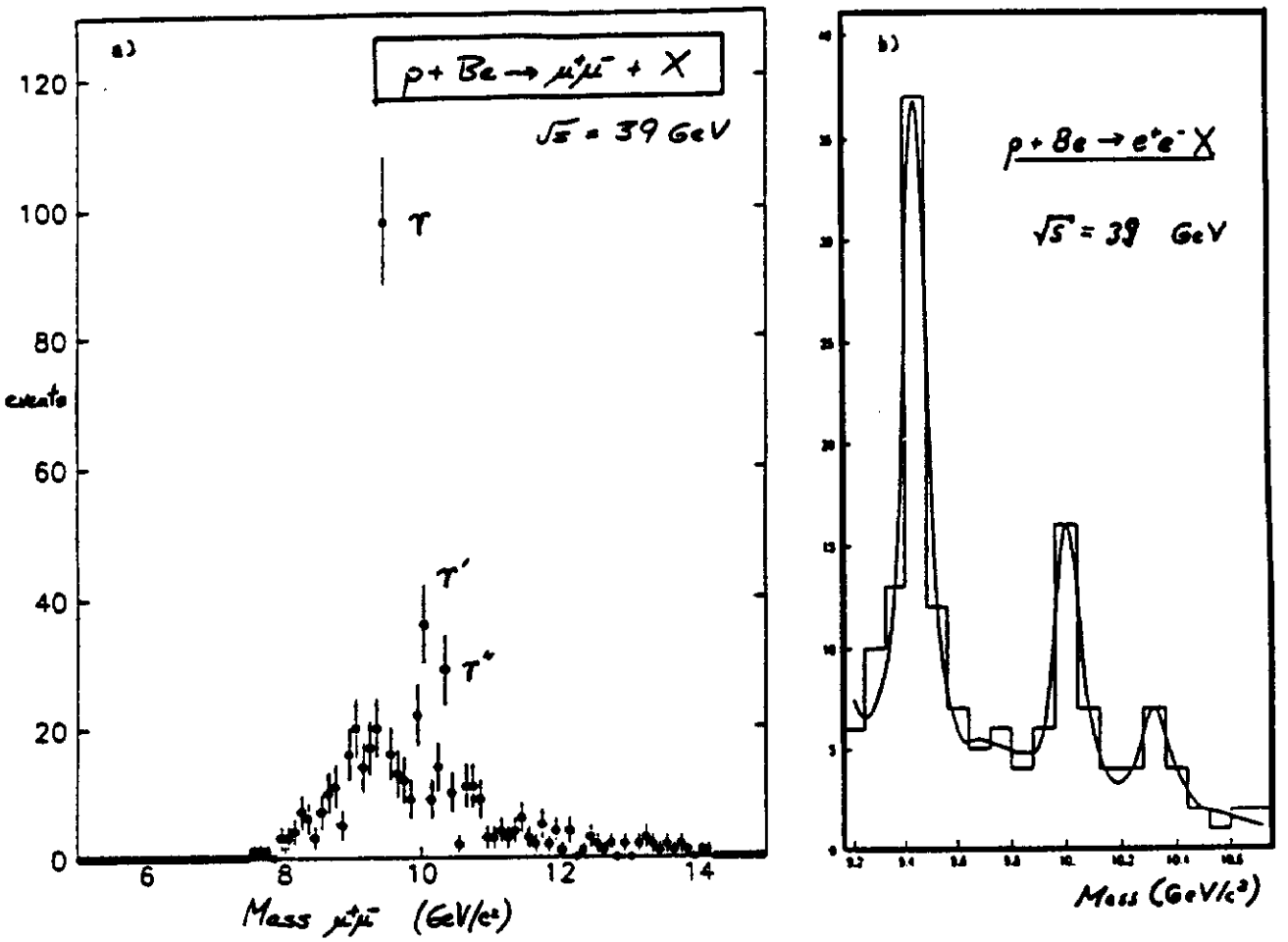

FIGURE 12: Yield of opposite-sign a) muon pairs and b) electron-positron pairs vs. mass at 800 GeV.

7.2 High-Luminosity Dimuon Run

In 1985 we added a 4'-thick Pb absorber at the exit of SM12 in order to eliminate our photon background (see Figure 13). We were thus able to increase our luminosity by a factor of 30. We retain good mass resolution (0.2% r.m.s. at the T) in the presence of the absorber, since SM3 provides a good measurement of momentum and we trace the trajectory back through the field of SM12 in order to determine the production angle, allowing the track to have a kink due to multiple scattering in the absorber. To improve the momentum determination we added a station of proportional drift tubes ("Station 0") just downstream of SM12, which we successfully operated at rates in excess of 100 MHz (2 MHz on the hottest wire). Using Station 0 SM3 provides 0.1% momentum measurement. Table 2 gives expected contributions to the mass resolution at the T.

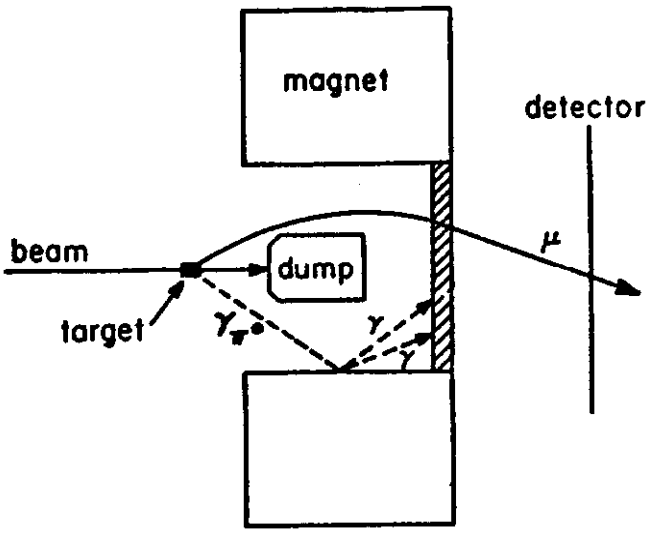

FIGURE 13: Schematic diagram of apparatus with Pb absorber installed.

TABLE 2: Expected Contributions to Closed-Aperture T Mass Resolution

Contribution	σ (MeV/c²)
target size	6.3
dE/dx fluctuations	3.0
multiple scattering	
in target	9.4
in lead absorber	7.8
in detectors	6.5
in helium	3.7
chamber resolution	7.0
other	4.6
TOTAL	18.0

Table 3 summarizes rates at various stages in the apparatus and data acquisition. In order for data acquisition not to be the limiting bottleneck, we used a two-stage trigger. The first stage consisted of a trigger matrix which looked for triple coincidences of hodoscopes pointing back to the target in the bend plane. The second stage was a fast parallel-pipelined trigger processor [14], which found wire-chamber tracks in the bend plane pointing back to the target and firing the muon proportional tubes and required two opposite-sign tracks with mass exceeding a threshold. The trigger processor not only reduced the trigger rate by an order of magnitude, but gained another order of magnitude in required off-line computing for those events written to tape, since chamber hits inconsistent with processor tracks could be ignored in the off-line trackfinding. (Due to the high beam intensity there were typically 10 to 20 accidental hits per chamber plane per event.) Figure 14 shows trigger processor efficiency; the inefficiency is consistent with that expected from chamber inefficiency and dead time.

TABLE 3: Rates per 2×10^{12} Protons on Target

(Closed Aperture, 800 GeV)

station 0	5×10^9
station 1	2×10^9
station 3	5×10^8
muon hodoscope left-right coincidences	10^6
trigger matrix coincidences	2×10^3
events satisfying trigger processor	2×10^2
good high-mass $\mu^+\mu^-$ events found off line	2

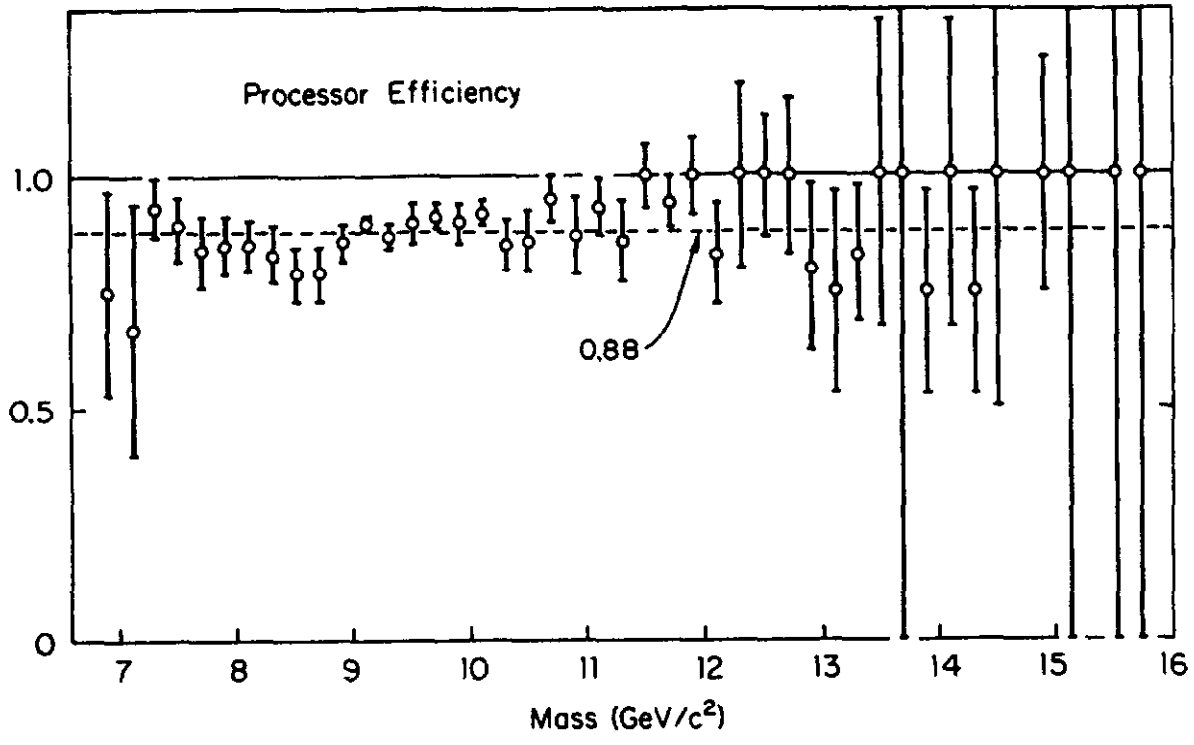

FIGURE 14: Trigger Processor Efficiency vs. mass.

Figure 15 shows event yield in the T region with half of the data analyzed. The mass resolution has not yet been optimized, but the three T states below B-meson decay threshold stand out clearly and with little background. Table 4 gives preliminary measurements of cross-section times branching ratio for production of T's. Using values measured at e^+e^- colliders for leptonic branching ratios [15], we can extract differential cross-section ratios for the three states, shown in Table 5. These have been predicted by Baier and Rückl [16] assuming T-production in 800-GeV pN collisions is dominated by gluon-gluon fusion into P states, which subsequently decay into the observed S states. Their predictions are also indicated in Table 5 and are in reasonable agreement with our result. Barger, Keung, and Phillips [17] and Childress et al. [18] used models based on local duality to calculate the sum of cross-section times branching ratio for all three T states. In these models the cross-sections are strongly sensitive to the shape of the gluon structure function. The T data pin down the gluon structure function to within one power of (1-x): Barger et al. find the exponent to be 5 or 6, while Childress et al. (who include $q\bar{q}$-annihilation in their analysis) find 7.6 ± 1.

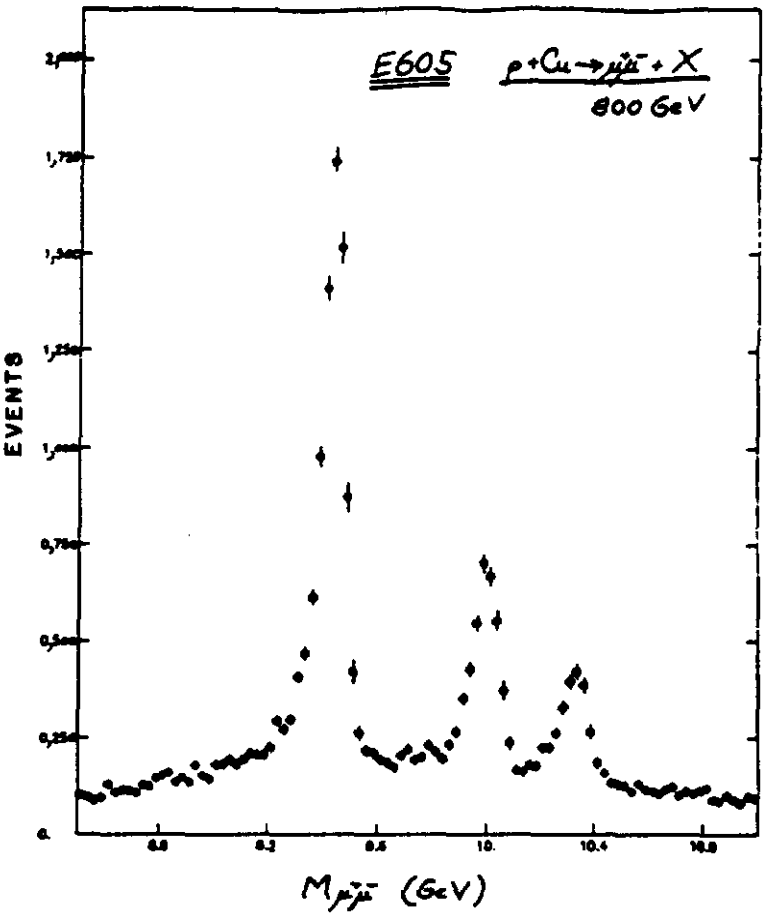

FIGURE 15: Yield of opposite-sign muon pairs vs. mass in the T region at 800 GeV off Cu for 1/2 of the closed aperture data.

TABLE 4: T Cross-Sections (Preliminary)

$p + Cu \rightarrow \mu^+\mu^- + X$ at 800 GeV

state	$B \left.\frac{d\sigma}{dy}\right\|_{y=0}$ (pb)
T (1S)	1.32 ± 0.08
T (2S)	0.36 ± 0.04
T (3S)	0.16 ± 0.02

TABLE 5: T B $\left.\frac{d\sigma}{dy}\right|_{y=0}$ Ratios (Preliminary)

$$p + Cu \rightarrow \mu^+\mu^- + X \text{ at } 800 \text{ GeV}$$

ratio	observed	predicted (Ref. 16)
T′/T	45 ± 8 %	$\lesssim$ 30 %
T″/T	16 ± 3 %	$\lesssim$ 15 %

Figure 16 gives the dimuon yield over the mass range 8 to 16 GeV/c^2. No new resonances are in evidence. Figure 17 shows 95%-confidence-level upper limits for the production of new resonances, expressed as a ratio to the Drell-Yan cross-section. These limits should come down a factor of two when the mass resolution has been optimized and the remainder of the data has been analyzed. Also shown are expected levels of signal for the Higgs [19] and the technipion [20], assuming they have masses in our accessible range. The Higgs production cross-section increases with the number of quark generations, assumed here to be four, and a plausible "k-factor" enhancement of two has also been put in.

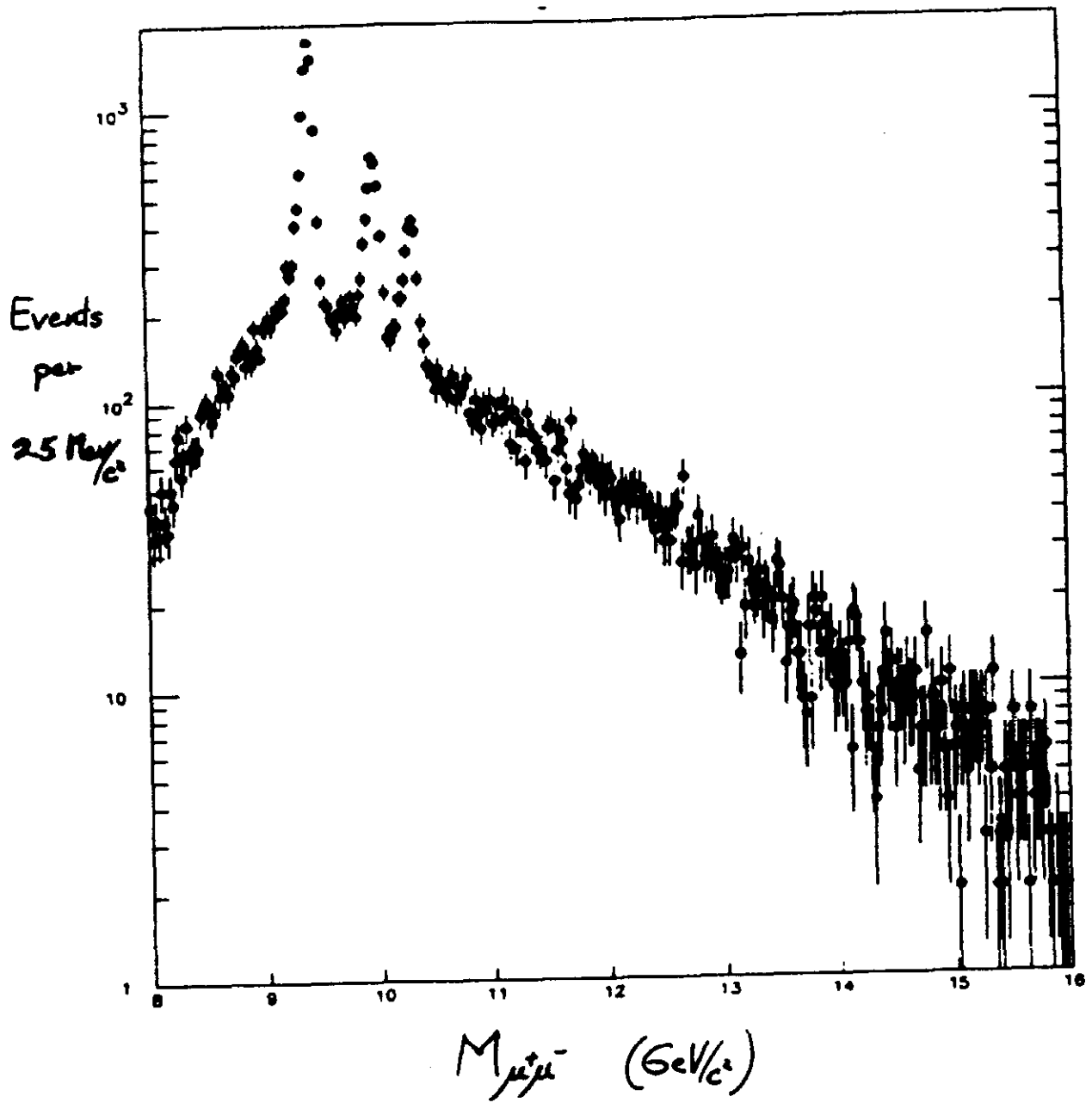

FIGURE 16: Yield of opposite-sign dimuons vs. mass at 800 GeV off Cu for 1/2 of the closed-aperture data.

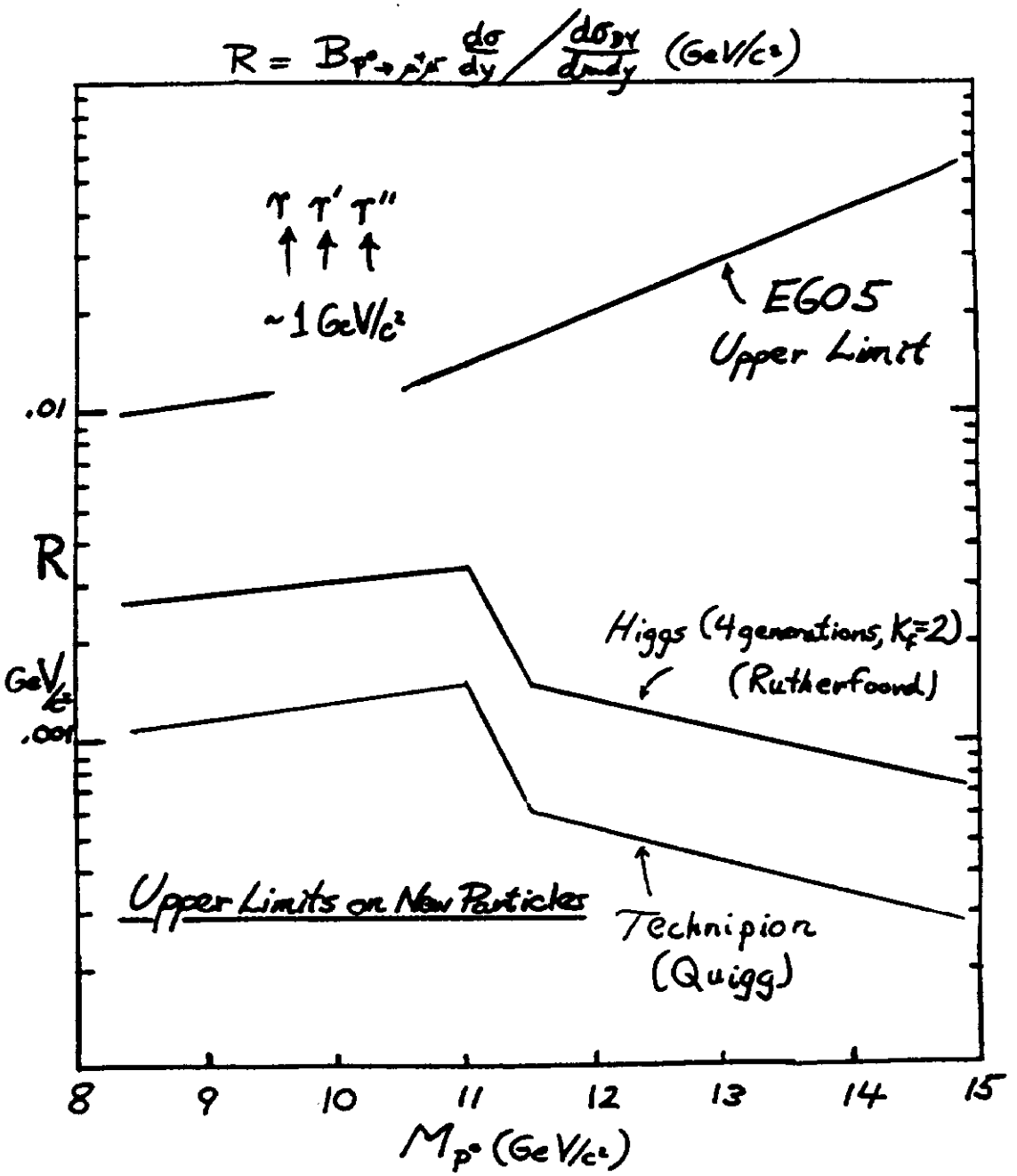

FIGURE 17: 95%-confidence-level upper limit vs. mass for dimuon resonance production cross-section times branching ratio, normalized to the Drell-Yan cross-section, and compared to predicted cross-sections for the Higgs and the Technipion.

7.3 Search for "Axions" [21]

Recently interest in axions has been renewed due to the observation of monoenergetic electrons and positrons produced in heavy-ion collisions [22], suggesting the production and decay of a particle with mass = 1.8 MeV/c^2. Our relatively short (5.5 m) Cu beam dump, located within the field of SM12, followed by a spectrometer with good electron identification turns out to give excellent sensitivity to such a particle, produced in a π^0-initiated electromagnetic shower at the upstream end of the Cu beam dump and decaying downstream of the dump.

We took a sample of data triggered only on energy deposition in the calorimeter during the 1984 800-GeV run, and for 4 x 10^{13} protons on target we find 74 e^+e^- pairs which reconstruct to a vertex at the downstream face of the dump. These pairs are all consistent with zero mass. Figure 18 shows the distributions of the exit angles of the pairs in the vertical and horizontal planes at the downstream face of the dump. During the same data runs we also recorded a prescaled sample of the copious flux of muons emerging from the downstream face of the dump. These muons were produced by meson decay in the initial hadron shower and were then deflected in the vertical plane due to the 3.1 GeV/c magnetic kick over the length of the dump. The angular distributions of the muons were identical to the distributions of the e^+e^- pairs in Figure 18. Axions, traversing the dump as neutral particles, would be expected to have narrow angular distributions in both x and y. The e^+e^- angular distributions are consistent with muon bremsstrahlung in the last radiation length of the beam dump, and at most one pair is consistent with the decay of a neutral particle produced at the upstream end of the dump.

Using a phenomenological fit to the flux of π^0's in thick targets [23] and an axion production formula due to Tsai [24] (assuming pseudoscalar coupling of the axion to e^+e^-), we can compute 90%-confidence-level limits on the mass and lifetime of the axion, shown in Figure 19. Also shown are limits vs. mass and lifetime derived from the anomalous magnetic moment of the electron [25], which would receive a large contributibution from axion loops if the axion-electron coupling becomes large. (These limits are not much different for other possible axion couplings.) Together the two measurements exclude a large region in mass-lifetime space, and a 1.8-MeV axion appears to be ruled out (unless it interacts strongly and is absorbed in the beam dump).

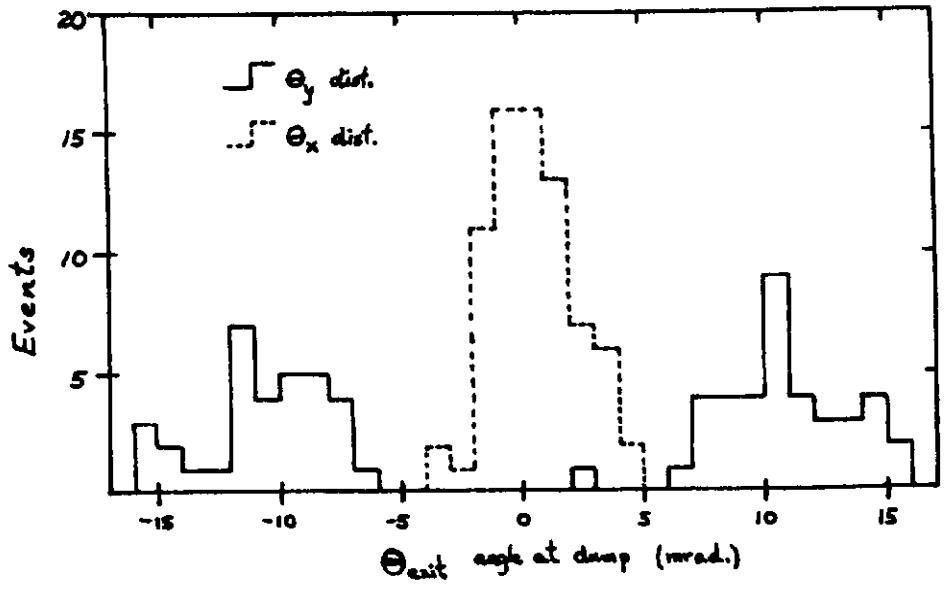

FIGURE 18: Exit angle distributions at the downstream dump face for the observed electron-positron pairs.

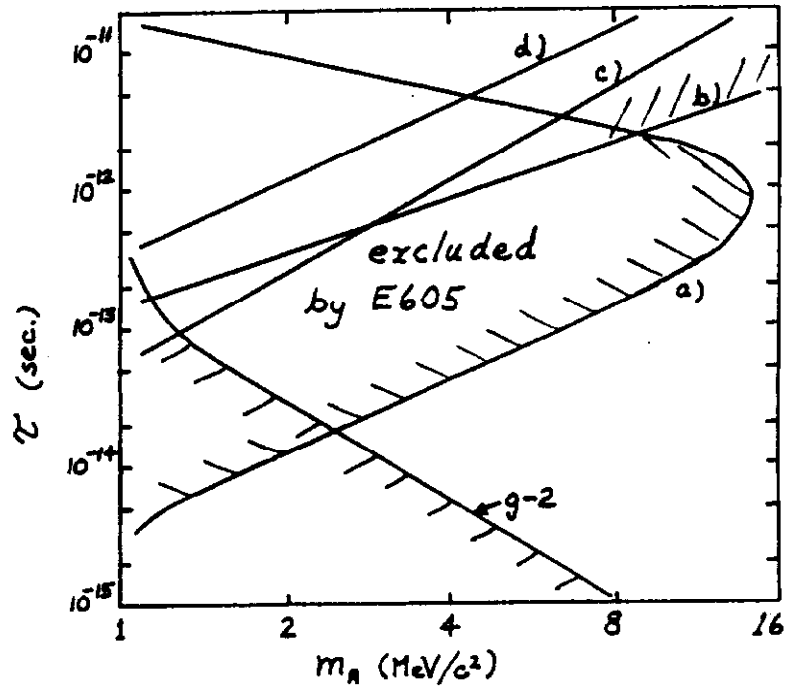

FIGURE 19: Limits on mass and lifetime of an axion-like particle from a) this experiment, and previously published limits from b) KEK, Konaka et al., c) FNAL E613, and d) SLAC E56. Also shown is the lower limit from g-2 measurements.

8 Acknowledgement

We thank our colleagues of the CERN-Columbia-Fermilab-Florida State-KEK-Kyoto-Saclay-Stony Brook-Washington collaboration, as well as the support staffs of the respective institutions, for their able work in carrying out Experiment 605.

NOTES

[†]E605 Collaboration: M.R. Adams, C.N. Brown, G. Charpak, S. Childress, W.E. Cooper, J.A. Crittenden, D.A. Finley, H.D. Glass, R. Gray, Y. Hemmi, Y.B. Hsiung, J.R. Hubbard, K. Imai, A.S. Ito, D.E. Jaffe, A.M. Jonckheere, H. Jöstlein, D.M. Kaplan, J. Kirz, L.M. Lederman, K.B. Luk, A. Maki, Ph. Mangeot, R.L. McCarthy, K. Miyake, G. Moreno, T. Nakamura, R. Orava, A. Peisert, R.E. Plaag, J.E. Rothberg, J.P. Rutherfoord, Y. Sakai, N. Sasao, F. Sauli, S.R. Smith, P.B. Straub, K. Sugano, N. Tamura, K. Ueno, R. Williams, T. Yoshida, K.K. Young

REFERENCES

1. D. Antreasyan et al., Phys. Rev. D19, 764 (1979).

2. H. Jöstlein et al., Phys. Rev. D20, 53 (1979);

   A.S. Ito et al., Phys. Rev. D23, 604 (1981);

   S.R. Smith et al., Phys. Rev. Lett. 46, 1607 (1981).

3. K. Ueno et al., Phys. Rev. Lett. 42, 486 (1979);

   D.A. Garelick et al., Phys. Rev. D18, 945 (1978).

4. E. Rutherford, Philosophical Magazine, ser. 6, xxi, 669 (1911).

5. H. Glass et al., IEEE Trans. Nucl. Sci. NS-32, 692 (1985).

6. J.A. Crittenden et al., "Inclusive Hadronic Production Cross-Sections Measured in Proton-Nucleus Collisions at $\sqrt{s}$ = 27.4 GeV," to appear in Phys. Rev. D (1986);

   Y. Sakai, Ph.D. thesis, Kyoto University (1984);

   H. Glass, Ph.D. thesis, SUNY at Stony Brook (1985);

   Y. Hsiung, Ph.D. thesis, Columbia University (1985);

   J. Crittenden, Ph.D. thesis, Columbia University (1985).

7. Y.B. Hsiung et al., Phys. Rev. Lett. 55, 457(1985).

8. R.L. McCarthy et al., Phys. Rev. Lett. 40, 213 (1978).

9. M. Lev and B. Petersson, Z. Phys. C21, 155 (1983).

10. T. Sjöstrand, private communication;

    T. Sjöstrand, Computer Phys. Comm. 27, 243 (1982).

11. J.F. Owens, private communication; see also D.W. Duke and J.F. Owens, Phys. Rev. D30, 49 (1984).

12. W. Bartel et al., Z. Phys. C20, 187 (1983).

13. A. Breakstone et al., Phys. Lett. 135B, 510 (1984) and CERN/EP 85-30, submitted to Z. Phys. C.

    T. Åkesson et al., Nucl. Phys. B246, 408 (1984).

14. Y.B. Hsiung et al., "Use of a Parallel Pipelined Event

Processor in a Massive-Dimuon Experiment," to appear in Nucl. Instr. & Meth. (1986).

15. Particle Data Group, "Review of Particle Properties," Rev. Mod. Phys. 56, No. 2, Part II (1984).

16. R. Baier and R. Rückl, Z. Phys. C19, 251 (1983).

17. V. Barger, W.Y. Keung, and R.J.N. Phillips, Z. Phys. C6, 169 (1980).

18. S. Childress et al., "Production Dynamics of the T and the Gluon Structure Function," unpublished, 1983.

19. J.P. Rutherfoord, private communication.

20. C. Quigg, FERMILAB-PUB-85/145-T.

21. C.N. Brown et al., "A Sensitive Search for the Axion," submitted to Phys. Rev. Lett. (1986).

22. J. Schweppe et al., Phys. Rev. Lett. 51, 2261 (1983);

M. Clemente et al., Phys. Lett. 137B, 41 (1984);

T. Cowan et al., Phys. Rev. Lett. 54, 1761 (1985) and Phys. Rev. Lett 56, 444 (1986).

23. A.J. Malensek, Fermilab preprint FN-341, FN-341-A.

24. Y.S. Tsai, SLAC-PUB-3926, April 1986.

25. S.J. Brodsky et al., Santa Barbara preprint NSF-ITP-86-17.